Zeitschrift: IABSE publications = Mémoires AIPC = IVBH Abhandlungen
Band: 1 (1932)

Artikel: Wind pressure on buildings
Autor: Nøkkentved, Chr.
DOI: https://doi.org/10.5169/seals-729

WIND PRESSURE ON BUILDINGS

ACTION DU VENT SUR LES BÂTIMENTS

WINDDRUCK AUF GEBÄUDE

Dr. sc. techn. CHR. NØKKENTVED,
Dozent an der Technischen Hochschule, Kopenhagen.

Although rapid development has taken place of late years in the realm of elasticity and statics, the foundations upon which they build have not, in many respects been developed to a corresponding extent.

A case in point is the pressure of wind on buildings; knowledge on this subject is still so small, that even at the present day it is quite impossible to formulate definite windpressure factors for use in calculations.

The passing years have witnessed a long series of windpressure experiments, but a surprisingly small number of these have been for the purpose of studying the pressure of wind on buildings. It was with the idea of adding something to the knowledge of this comparatively little cultivated field that Dr. IRMINGER and the author in 1927 commenced a series of systematic investigations. In the following, some of the results obtained will be briefly discussed, recourse being had, on certain points, to the work of other investigators. Most of the experiments have been dealt with in an earlier publication [1]), while the streamflow illustrations and the pressure distribution experiments in connection therewith are here made public for the first time.

Wind is not a uniform flow of air, but an ever shifting series of vortices borne in the main stream, and causing the velocity and direction to be continually changing. For this reason measurements made in the natural wind give an extremely complicated and obscure picture of the conditions. Investigations must, therefore, be carried out with models in a windchannel in which a completely uniform windstream has been secured.

The nature of windpressure having in this way been ascertained, further investigations will have to be undertaken to determine the influence of variation in the velocity of the wind, i. e. gusts.

As is known, windpressure is ordinarily proportional to the square of the velocity, the pressure being chiefly due to the air's energy of motion, which can be expressed as $\frac{1}{2} \varrho v^2$ (This expression has by Dr. Irminger and the author been termed a "newton" and written nt) [1]).

For atmospheric air $nt = 0{,}0625\ v^2$ where v is the velocity in metres per second. Pending more exact measurement, one may calculate with a maximum wind velocity of 40 m/sec so that $nt = 100$ kilogram/m^2.

Friction between the air and the body in the windstream introduces a disturbing factor into the otherwise constant relationship between wind-

[1]) Wind-pressure on Buildings by IRMINGER and NØKKENTVED; Ingeniørvidenskabelige Skrifter A, No. 23, Copenhagen 1930.

pressure and nt. The English physicist REYNOLDS has, however, shown that for geometrically similar bodies there will also be mechanical similarity when the so-called Reynolds' number $R = \frac{v\,d}{\nu}$ is similar; v is the wind velocity, d a linear dimension for the body and ν is the viscosity. For atmospheric air at 15° C. and 760 mm ν may be taken at 0,145 cm²/sec. With a cylinder, for instance, the pressures, in proportion to nt will be the same, at all points, even if the diameter be doubled provided only that the velocity is reduced to the half.

In the following, all windpressures are expressed as a fraction of nt, and are given both as the pressure upon unit surface, and as the total resistance figure c; the total windpressure can therefore be found by the formula $P = c \cdot F : nt$, where F is the projected area of the building at right angles to the direction of the wind.

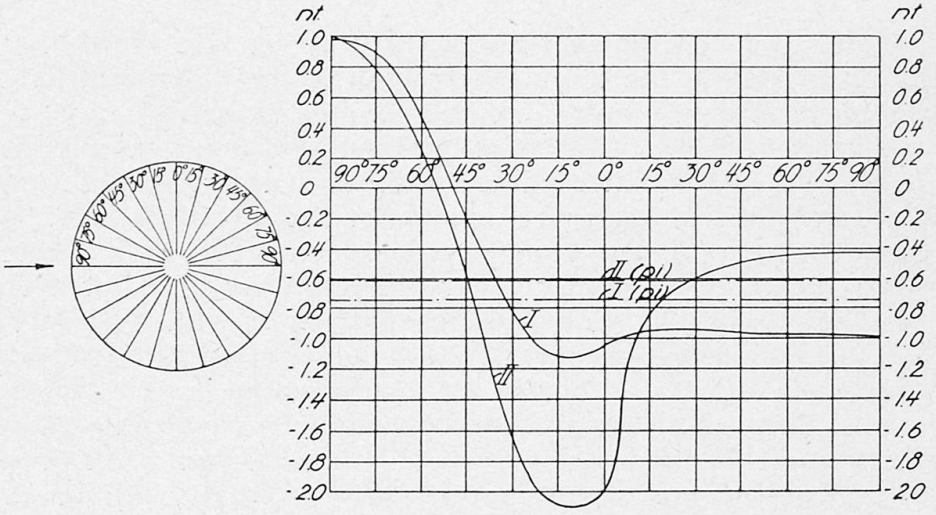

Fig. 1.
Cylinder, Pressure Curves — Cylindre, courbes des pressions — Zylinder, Druckverteilungskurve.

It should be mentioned, further, that in order to determine the actual pressure upon a unit of area at a given point upon a building, not only must the external pressure be known, but also the internal pressure; the effective pressure being the difference between them. Investigation has shown that the internal pressure is directly dependant upon and proportional to the external pressure, further, that one may assume the same internal pressure anywhere in an inside room. On the other hand, the internal pressure depends, of course, upon the distribution of the leakage between the inside of the building and the outer air, not particularly, however, upon the size of the leaks or openings. To give a general idea of internal pressure, this is stated in all cases for buildings with a uniform permeability.

1. Cylinders.

(Water Standpipes, Smokestacks, Stays, Wires etc. etc.)

In Fig. 1 the case of a cylinder of infinite length is presented; to the right, pressure curves are drawn on the opened out half-cylinder. It is seen that there is positive pressure on the leading arc of the cylinder, but 35° to the right and left of the 90° point the pressure has already changed to ne-

gative pressure, which reaches a maximum 10°—15° from 0°. Two curves are shown; I for a Reynolds' number of 10000 and II when $R = 500000$. The former will, under practical conditions, correspond to a diameter $d < 4$ cm and the latter to $d > 15$ cm. The internal pressure is shown by the stippled lines and is seen to be negative; for curve I, $p_i = -0{,}75\ nt$ and for II $p_i = -0{,}62\ nt$.

Fig. 2 is plotted with the resistance figure c as ordinates and Reynolds number as abcissae. One will notice the great and sudden drop in c when $R = 500{,}000$ corresponding to the difference between the two curves of Fig. 1 and due to friction completely altering the streamflow conditions, when the wind velocity or the dimension of the cylinder results in the above value of R.

The curve of Fig. 2 shows that when $d < 4$ cm, c can be put at about 1,1 and when $d > 15$ cm, $c =$ about 0,4. The former must therefore be used

Fig. 2.

Cylinder, Resistance figure c for different Reynold' numbers.

Cylindre, coefficients de résistance c pour des constantes differentes de Reynold.

Cylinder, Widerstandszahl c für verschiedene Reynoldsche Zahlen.

for Stays, Wires and the like, and the latter for Smokestacks, Water towers etc. All the figures given apply to cylinders of infinite length; for those of finite length the value will be somewhat lower, a matter, however, of little significance until heights become less than 1,5 times the diameter; for such short cylinders no measurements are available.

Upon the flat top of the cylinder the suction, at any rate where the height $= h > 1{,}5\ d$, can be taken at about 80 % of nt.

2. Prisms.

Fig. 3 presents a square prism with a height $h = 2{,}5$ times the length of side a. Pressure curves are shown for four angles of incidence and three elevations. It is seen that negative pressures predominated, and that at an angle of incidence of 75° a praticularly powerful suction is found at the leading edge, attaining a value of $-1{,}7\ nt$.

For square prisms with other proportions of $h:a$ the pressure curves are quite similar to those given, but with other ordinates. Some figures for the prisms we have examined viz. with $h:a$ ratios of 1 (a cube); $h:a = 2{,}5$ (the above mentioned prism, which is very similar to the model of a skyscraper examined by the Bureau of Standards, Washington), and $h:a = \infty$ (an infinitely long prism) are given in the accompanying table.

The resistance figure c' must first be multiplied by the area of a side (not the projected area of the prism on a plane at right angles to the wind) and by nt (which as previously stated may be put at 100 kg/m²) to give the total horizontal resistance.

$\frac{h}{a}$	Angle of incidence 90°						
	c'	p_A	p_B	p_C	p_D	p_E	p_i
1	1,05	+ 0,76	— 0,62	— 0,29	— 0,62	— 0,65	— 0,41
2,5	1,30	+ 0,80	— 0,67	— 0,50	— 0,67	— 0,68	— 0,43
∞	1,90	+ 0,79	— 1,32	— 1,11	— 1,32		— 0,50

$\frac{h}{a}$	Angle of incidence 45°						
	c'	p_A	p_B	p_C	p_D	p_E	p_i
1	1,13	+ 0,39	— 0,41	— 0,41	— 0,39	— 0,53	— 0,19
2,5	1,35	+ 0,45	— 0.50	— 0,50	— 0,45	— 0,60	— 0,05
∞	2,10	+ 0,40	— 1,10	— 1,10	— 0,40		— 0,35

The average external pressure on the four sides (*A, B, C, D* of Fig. 3) are given as p_A, p_B, p_C, p_D; the average external pressure on the roof plane as p_E, and the internal pressure as p_i, all in proportion to nt.

It will be noticed that the total horizontal resistance is very nearly the same at 45° as at 90° angle of incidence; further, that the resistance figure c' increases from 1,1 for $h:a = 1$, to 2,0 for $h:a = \infty$, the reason apparently being that while the positive pressure remains constant, the negative pressure more than doubles.

3. Building types.

The experiments carried out up to the present can be broadly placed in 2 main groups. The first embraces building models 50 mm high to eaves, 50 mm wide, and 100 mm long, with roof pitches of 0°, 20°, 30°, 40°, 45° and 60°. Measurements were made on side walls, end walls, and roofs and for angles of incidence of 90°, 75°, 60°, 45°, 30°, 15°, and 0° (90° is with the wind at right angles to the length of the building, and 0° at right angles to an end). The second group comprises buildings that may be considered of infinite length in that they were at both ends bounded by large screens which cut off all side flow, and ensured two-dimensional flow conditions. In addition to building types of the first group, placed between the screens, a special series of experiments were carried out with a building in which the roof pitch was variable from 0° to 35° in 5° steps. Parallel with these experiments the author carried out, at Göttingen, the stream flow experiments to be described.

a) First group of experiments. Fig. 4 presents some typical results; on the plan view the sides, ends and roof surfaces are lettered for later reference and the various angles of incidence indicated. Four sets of cross sections of the buildings are also shown, one set for each angle of incidence, and on each section, curves are drawn showing the pressures at the three positions I, II and III on plan. The ordinates of these curves give the difference between the external and internal pressures.

The mean pressure is written opposite each surface, while below each section the internal pressure p_i and the pressures on the end wall p_B and p_D are given.

On the whole the figures are self-explanatory, but it is worth while drawing attention to the characteristic differences between the curves for the windard roof surface *E* (90° angle to the wind); this is still more clearly

seen in the 2nd. group of experiments and in the account of these, an explanation of the phenomenon will be given.

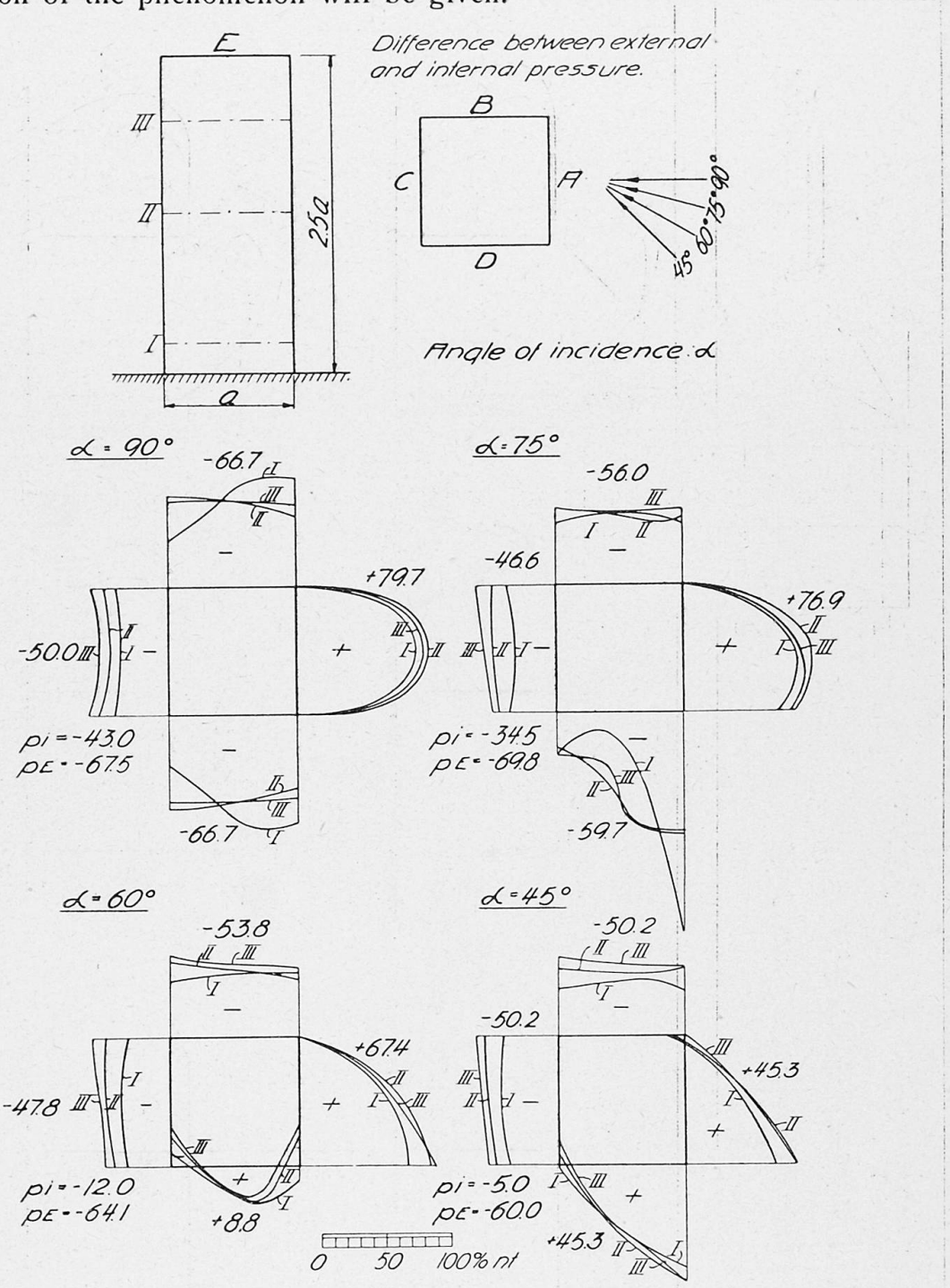

Fig. 3.

Prism, Pressure curves and average pressures — Prisme, courbes des pressions et pressions moyennes — Prisma, Druckverteilungskurven und mittlere Drücke.
Difference between external and internal pressure — Différence entre les pressions intérieure et extérieure — Differenz zwischen Innen- und Außendruck.
Angle of incidence — Angle d'incidence — Einfallwinkel.

When one compares the values for suction with those for internal pressure given in Fig. 4, one realises that in the question of the stability of a roof the internal pressure plays a large part. Internal pressure is always negative

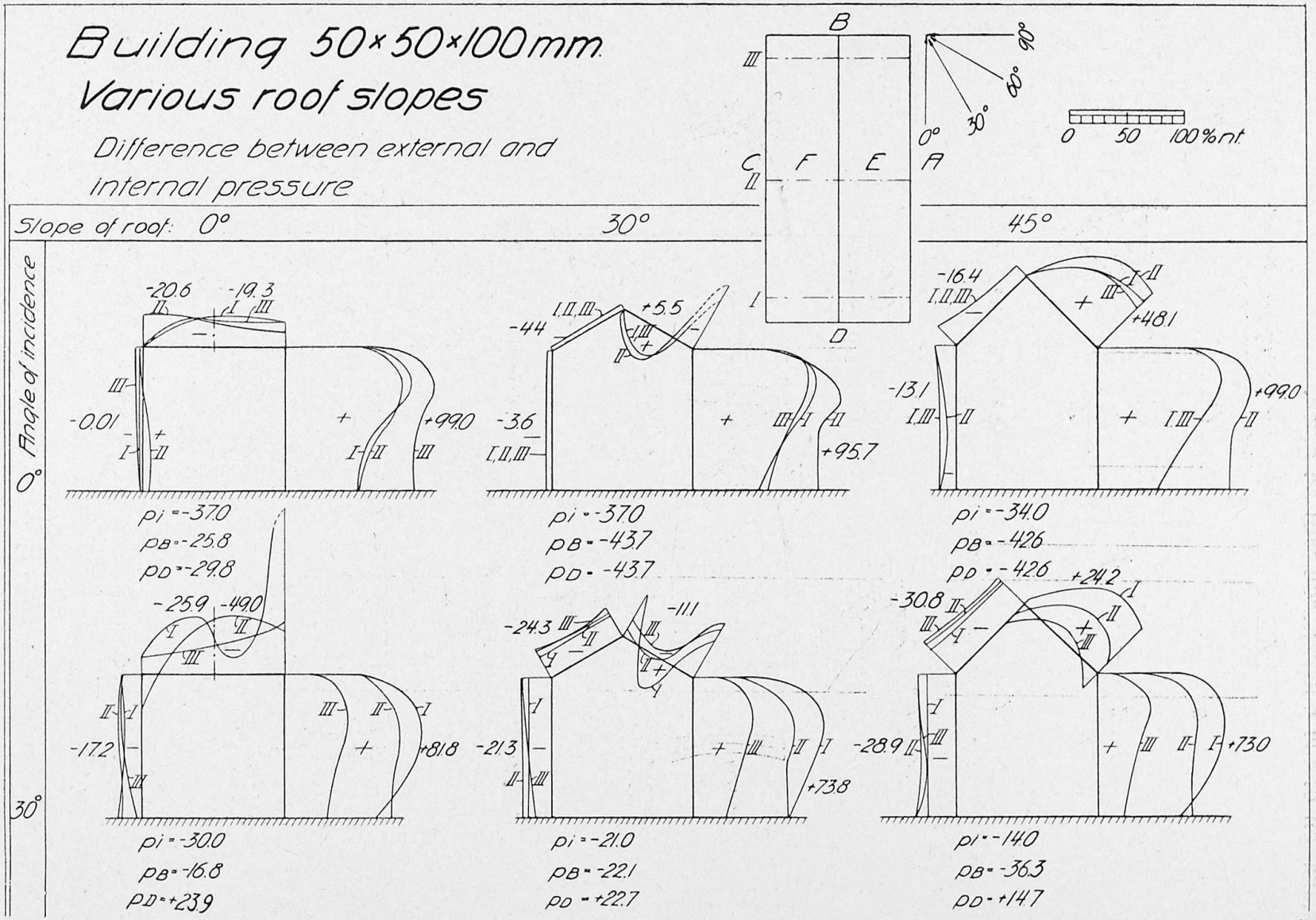
Building 50×50×100mm.
Various roof slopes
Difference between external and internal pressure
B
C
F
E
A
D
0°
30°
90°
0 50 100% nt.
Slope of roof: 0° 30° 45°
Angle of incidence
0°
30°
-20.6 -19.3 -0.01 +99.0
pi = -37.0
pB = -25.8
pD = -29.8
-44 -3.6 +5.5 +95.7
pi = -37.0
pB = -43.7
pD = -43.7
-16.4 +48.1 -13.1 +99.0
pi = -34.0
pB = -42.6
pD = -42.6
-25.9 -49.0 -17.2 +81.8
pi = -30.0
pB = -16.8
pD = +23.9
-24.3 -11.1 -21.3 +73.8
pi = -21.0
pB = -22.1
pD = +22.7
-30.8 +24.2 -28.9 +73.0
pi = -14.0
pB = -36.3
pD = +14.7

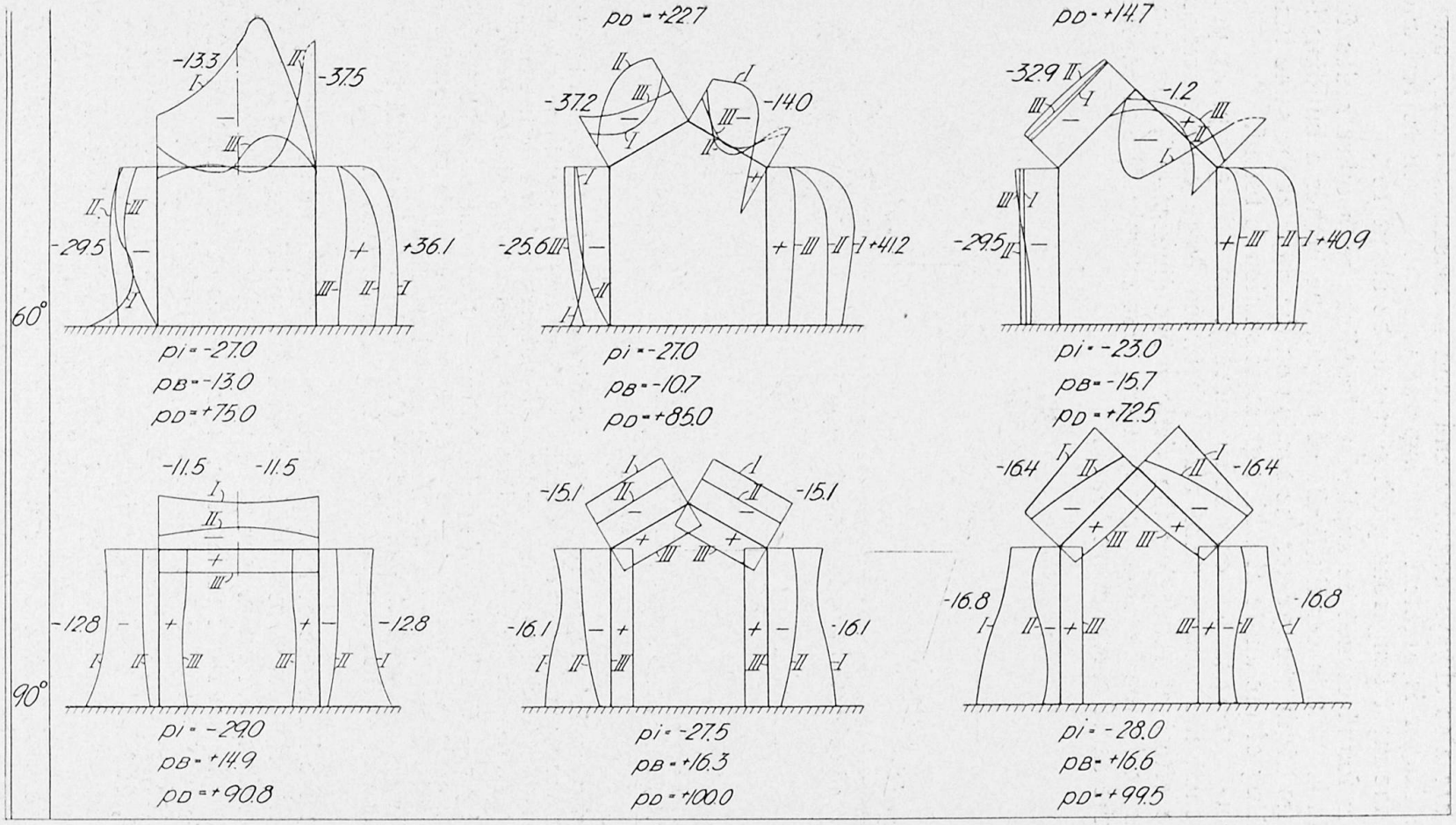

Fig. 4.

Building 50 × 50 × 100 mm with various roof slopes and angles of incidence — Bâtiment de 50 × 50 × 100 mm avec des inclinaisons de toiture et des angles d'incidence différents — Gebäude 50 × 50 × 100 mm mit verschiedenen Dachneigungen und Einfallswinkeln.

Various roof slopes — Différentes pentes de toit — Verschiedene Dachneigungen.

Slope of roof — Pente du toit — Dachneigung.

Difference between external and internal pressure — Différence entre les pressions intérieure et extérieure — Differenz zwischen Innen- und Außendruck.

Angle of incidence — Angle d'incidence — Einfallwinkel.

and tends therefore to hold the roof on, but the external pressures for pitches less than 40° are also always negative and tend to loosen and carry away the roof. The danger is greatest with impermeable roofs such as felt and copper, while the most dangerous pitch seems to be about 10°.

The values found cannot be applied to buildings with other ratios for height and width. Within certain limits of height, the higher a building in proportion to its width, the greater the suction on the roof; at the same time there is a shifting of the angle at which greatest suction is found.

b) Second group of experiments[2]). In this group, as previously mentioned the models were placed between large cut-off screens which had the effect of rendering the airflow two-dimensional, the same building types as in the previous group were first examined, and at 90° substantially the same curves were found.

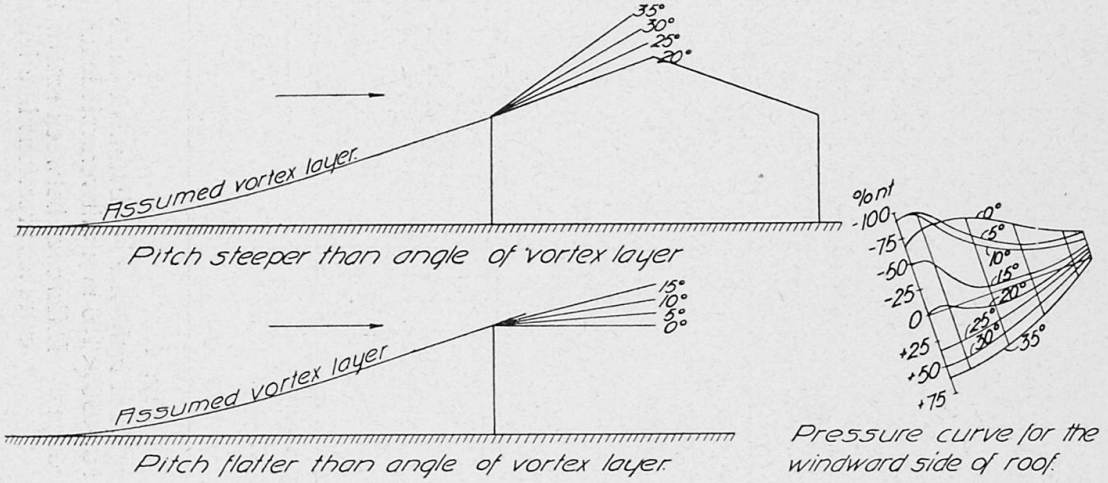

Fig. 5.

Building with various roof slopes, pressure curves for windward roof side, assumed vortex layer — Bâtiment avec des inclinaisons de toiture différentes, courbes des pressions sur le toit, côté du vent, couche des tourbillons estimée — Gebäude mit verschiedenen Dachneigungen, Druckverteilungskurven für die Windseite des Daches, gedachte Grenzschicht gezeigt.

Assumed vortex layer — Couche supposée de tourbillons — Angenommene Wirbelschicht.
Pitch steeper than angle of vortex layer — Pente plus forte que l'angle de la couche — Neigung kleiner als der Winkel der Wirbelschicht.
Pressure curve for the windward side of roof — Courbe des pressions sur le toit, face au vent — Druckverteilung für die Windseite des Daches.

To enable the influence of roof pitch to be examined more closely, the next series of experiments were carried out with the building shown in Fig. 5, having an adjustable roof pitch. The pressure curves found for the windward slope are shown to the right of the Fig. For pitches of 35°, 30° and 25°, the pressure is positive over the whole area, at 20° it is about to change over to negative, and at 15° the change is complete. It is seen that for pitches of 15°, 10° and 5° the negative pressures make themselves felt for the most part on the area bordering the eaves, while with a pitch of zero the pressure becomes more equally distributed, and decreases at the eaves.

In order to arrive at a better understanding of these conditions the author carried out, in Göttingen, some stream flow experiments some of which are illustrated in Figs. 6 and 7.

---

[2]) A detailed account of these experiments will be published later.

The photographs were obtained in the following manner. A model lying on its side and fixed to a carriage was drawn through the water in a 60 × 60 cm channel. The model projected 5 mm above the surface of the water, and a horizontal cut-off plate under the submerged gable wall rendered the stream flow two-dimensional. The ground was represented by a long vertical plate, fastened to the model and moving with it.

Aluminium powder was dusted on to the surface of the water and when the carriage bearing the model was drawn through the water a picture of the stream flow was produced; a film camera mounted on the carriage recorded the picture. The photographs here shown were taken with an exposure

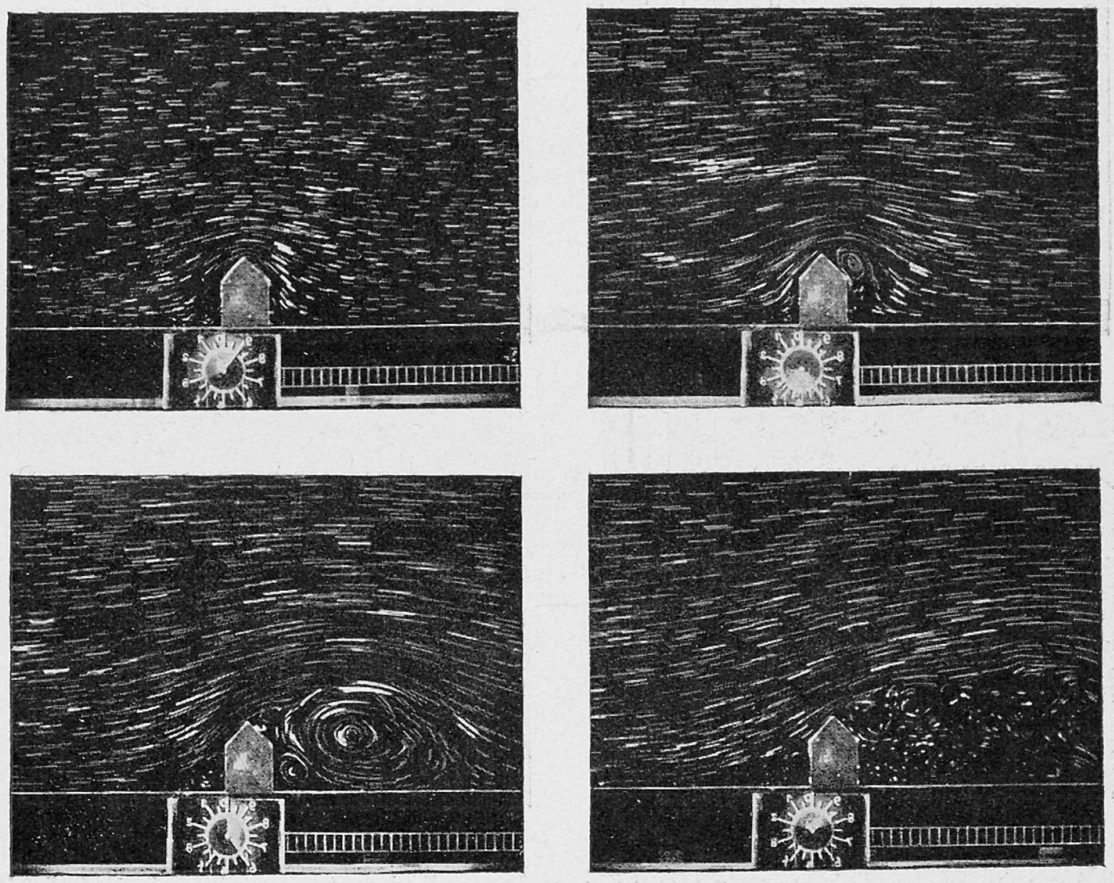

Fig. 6.
Building with 45° roof slope, streamflow illustration — Bâtiment avec toiture inclinée à 45°, graphique des lignes de courant. — Gebäude mit 45° Dachneigung, Stromlinienaufnahme.

of 1/3rd second, as indicated on the seconds dial seen in the illustration, the hand making one revolution per second. With this exposure the moving grains of aluminium appear as lines, and the length of the lines may be utilised as a measure of velocity.

The illustrations of Fig. 6 show the flow about a house 50 mm square with a 45° roof pitch. At the beginning of the flow the stream endeavours to follow the contour of the house, but the consequent constriction of the stream at the ridge gives rise to a high velocity and therefore a considerable velocity difference between adjacent stream lines. Friction in the fluid and at the surface of the body will result in an eddy; this will, as is seen, grow, and eventually flow away, drawing after it a vortex layer coming from the

ridge and made up of small vortices produced by friction at the surface of the body. No new large vortex will be created, as the layer, in an easy curve, will form a boundary surface to the dead water region at the back of the building, and over which the air stream will smoothly flow; in other words a streamline "body" is formed with the vortical layer as its surface. A mathematical investigation of the phenomenon fully justifies this view.

The dead water region in the rear of the building will be filled by the particles carried in by the first large vortex, and friction will cause them to

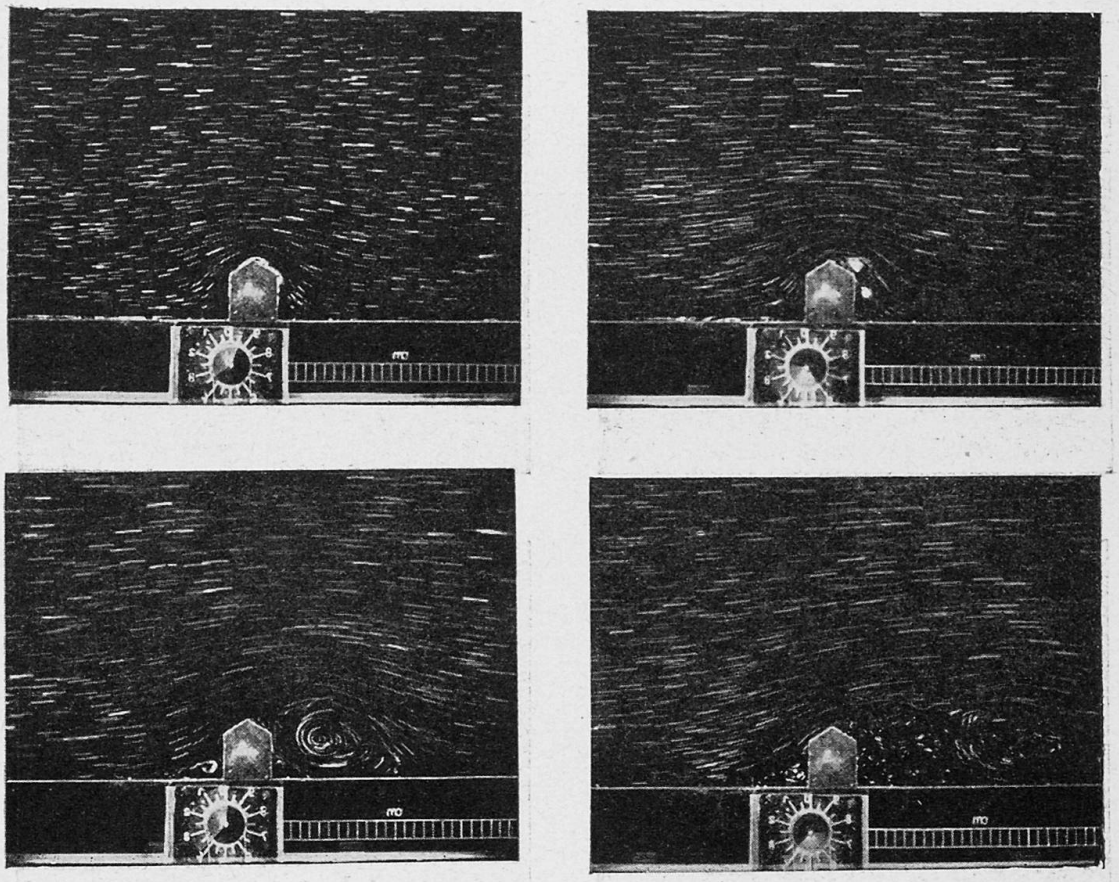

Fig. 7.

Building with 30° roof slope, streamflow illustration — Bâtiment avec toiture inclinée à 30°, graphique des lignes de courant — Gebäude mit 30° Dachneigung, Stromlinienaufnahmen.

gradually lose their velocity; a loss of energy which will express itself in the form of negative pressure.

In the same way, and for the same reasons as above, a dead water region will form at the front of the building, divided from the air stream by a vortex layer stretching in an easy curve from the "ground" to the windward eaves.

Observations of the illustrations in Fig. 7, of the conditions for a building with a 30° roof pitch, show that the phenomena for the 45° roof of Fig. 6 are repeated but with the important difference that while the slope of the vortex layer on the windward side of the house in Fig. 6 is flatter than the roof slope, in Fig. 7 it is steeper. With the 45° roof this will result in an upward sweep in the line of the flow at the windward eaves, causing a diminished velocity and consequently positive pressure. The 30° roof, on the other hand, will cause a downward bend, i. e. negative pressure.

These experiments afford a physical explanation of the various pressure curves of Fig. 5, in which the assumed vortex layer curves have been drawn in. It should here be remarked that the ratio of height to width is not the same as for the model in the stream flow experiments, the corresponding roof pitches will not therefore, give rise to corresponding phenomena; the 30° roof, in the stream flow experiments, will in effect most nearly correspond to the 10° slope in Fig. 5. The assumed vortex layer slope in Fig. 5 is flatter than the roof slope for 35°, 30°, 25° and 20° pitches and corresponds to the positive pressure found, while for 15°, 10° and 5° the vortex layer path must be steeper, the difference in angle is, however, so little that only a very limited dead water region is formed on the roof near the eaves; there is insufficient "elbow room" as it were, for the formation of a proper eddy; the stream flow hugs the roof surface closely, bending sharply at the eaves and thus setting up a powerful suction which, however, rapidly falls to a low value. With a pitch of 0° the vortex layer is of course steeper than the roof, but there is now formed a wide dead water region over the whole roof, the bend in the line of flow becomes easier and suction at the eaves, therefore, less but on the other hand spread over a greater portion of the roof area.

Hitherto, attention has only been paid to the vortex layer at the rear of the building, and while for round bodies one can conceive the layer breaking away at many different points, for sharp edged bodies it will always issue from well defined points such as a roof ridge. It has been thought, therefore, that experiments with models could be directly applied to full size buildings, but the presence of the vortex layer to windward of the building having been ascertained, it is to be expected that the size of model, in the case of sharpedged bodies, such as buildings will also have to be taken into account although probably only for low roof pitches.

We have, as a matter of fact, found the above to be the case, but our final investigations into this matter are only at the commencement. So much, however, is certain, that the greatest caution must be excercised in applying the results of model experiments to full sized buildings, when the low roof pitches are in question. The problem is further complicated by the ever-changing velocity of the natural wind.

The experimental work already done has yielded a great deal of data upon the nature of wind, but it has also made clear that wind pressure on buildings is such a complicated and little explored subject that a very great deal of experimental work must yet be done before one can hope to prescribe definite rules for windpressure loads.

Summary.

In order to contribute to the knowledge of this little cultivated field, Dr. IRMINGER and the Author commenced in Copenhagen a long series of experiments with models in a wind tunnel.

All pressures are given in proportion to the kinetic energy of the wind, which per m³ can be expressed as $\frac{1}{2} \varrho v^2$, termed in this paper a "newton" and written *nt*. For atmospheric air and a velocity of 40 m/sec, $nt = 100$ kg/m².

Fig. 1 shows the pressure distribution upon an infinitely long cylinder. Curve I corresponds to a Reynolds number of $R = 10{,}000$ ($R = \frac{v d}{\nu}$: v = wind velocity, d = a linear dimension for the body and ν = viscosity = 0.145 cm²/sec). Curve II corresponds to a Reynolds number of $R = 500{,}000$.

Fig. 2 shows the total resistance figure C for various values of R. The total wind resistance is given by the formula $P = c \cdot F \cdot nt$.

Fig. 3 shows the distribution of pressure in the case of a square prism; the table gives the average pressure, resistance figure, and internal pressure for different prism heights and uniform premeability.

Fig. 4 shows some of the results obtained with various building types; all pressures are given as the difference between the external and internal pressures.

Fig. 5 presents pressure curves for various roof pitches and a slightly different type of building having cut-off screens at each end rendering the air flow two dimensional, it is seen that the 20° pitch forms the dividing line between the flatter pitches with negative pressure, and the steeper, upon which the pressure is positive.

To throw light upon these conditions the author carried out stream flow experiments in Göttingen, using, however, the building type of Fig. 4; a 40° roof in this case divides the negative pressure cases from the positive ones.

Fig. 6 and 7 illustrate the commencement and development of the flow conditions, for both a 45° and a 30° roof. It is seen how an eddy forms at the ridge and how this rolls away. It will also be observed that stable conditions are finally formed, with a vortex layer at the front of the building sweeping from the ground up to the eaves, and another streaming away to the rear from the ridge.

The vortex layer at the front of the building explains the differences in the above mentioned pressure curves. With a roof pitch of 45° the vortex layer slope is flatter than the roof slope and pressure on the roof results. At 30° the vortex layer slope is steeper than the roof slope causing suction on the roof. Following these lines, a supposed front vortex layer is drawn in on Fig. 5.

Hitherto attention has only been paid to the rear vortex layer with the belief, therefore, that experiments with sharp edged models could be directly applied to practice; the presence of the front vortex layer, however, renders it probable that the size of the model influences the distribution of pressure of the flatter roof pitches. As a matter of fact this has been found to be the case, and is now being investigated.

Résumé.

Pour contribuer aux recherches dans ce domaine peu étudié, M. le docteur IRMINGER et moi avons fait à Copenhague une longue série d'essais sur des modèles placés dans un canal de vent.

Toutes les pressions indiquées sont mesurées par rapport à l'énergie cinématique de l'air, qui peut être exprimée pour un mètre cube par l'expression $\frac{1}{2} \varrho v^2$. Cette expression est désignée par un „newton", qui s'écrit nt, et pour l'air atmosphérique et une vitesse du vent de 40 m/sec. elle peut être évaluée à $nt = 100$ kg/m².

La figure 1 indique la répartition de la poussée du vent sur un cylindre infiniment long. La courbe I correspond au chiffre de Reynolds 10 000 ($R = \frac{v d}{\nu}$, où v est la vitesse du vent, d une mesure linéaire du corps en question, et $\nu = 0{,}145$ cm²/sec est la viscosité), tandis que la courbe II correspond à $R = 500\,000$.

La figure 2 indique le coefficient de résistance total c pour les différentes valeurs de R. La résistance totale P se calcule par la formule $P = c \cdot F : nt$.

La figure 3 donne la répartition de la poussée pour un prisme carré, et le tableau indique pour des hauteurs différentes du prisme la pression moyenne, le coefficient de résistance et la pression intérieure (pour un corps uniformément perméable).

La figure 4 présente quelques résultats des essais faits sur des types différents de maison. Toutes les pressions sont indiquées comme la différence entre la pression extérieure et la pression intérieure.

La figure 5 enfin, reproduit des courbes de pression pour différentes inclinaisons de toiture et un autre type de bâtiment, limité aux bouts par des coupe-vent rigides, ce qui limite le courant à 2 dimensions. On voit que l'inclinaison de toiture à 20 degrés constitue la limite entre les toitures peu inclinées sur lesquelles l'action du vent exerce une succion, et les toitures à forte pente, sur lesquelles le vent exerce une pression. Pour trouver l'explication de ces courbes, j'ai fait à Goettingue des études sur les lignes du courant avec le type de maison de la figure 4, où les phénomènes analogues se groupent autour de la limite d'inclinaison de la toiture à 40°.

Les figures 6 et 7 montrent comment le courant s'établit tant pour l'inclinaison de 45° que pour celle de 30°. On voit comment, au faîte, se forme un tourbillon qui roule de la toiture, et qu'à l'état stationnaire il s'est formé une couche de tourbillons devant la maison s'étendant jusqu'à l'avant-toit antérieur et une autre couche de tourbillons derrière la maison commençant au faîte. La première couche de tourbillons explique les courbes des pressions susmentionnées: Pour une inclinaison de toiture de 45° la couche de tourbillons est moins inclinée que le rampant, tandis qu'elle est plus rapide pour l'inclinaison de 30°. Il en résulte de la pression sur le toit à 45° et de la succion sur celui à 30°. Conformément la figure 5 indique une importante couche antérieure de tourbillons.

Jusqu'à maintenant on ne s'est occupé que de la couche postérieure de tourbillons et on a cru, par conséquent, pouvoir appliquer à la pratique les essais sur modèles. La constatation de l'existence d'une couche antérieure de tourbillons rend vraisemblable l'hypothèse que les dimensions du modèle exercent une influence sur la répartition des pression pour certaines inclinaisons de toiture peu fortes. Cette influence sera étudiée de plus près.

Zusammenfassung.

Um einen Beitrag an die Untersuchung dieses wenig erforschten Gebietes zu leisten, haben Dr. IRMINGER und der Verfasser in Kopenhagen eine lange Reihe von Versuchen unternommen, die als Modellversuche in Windkanälen durchgeführt sind.

Alle Drücke sind im Verhältnis zu der kinetischen Energie der Luft, die pro m³ als $\frac{1}{2} \varrho v^2$ ausgedrückt werden kann, angegeben.

Diese Größe wird ein „newton", nt, genannt, und sie kann für atmosphärische Luft und für die Windgeschwindigkeit 40 m/sec als $nt = 100$ kg/m² festgestellt werden.

Fig. 1: Druckverteilung auf einem unendlich langen Zylinder. Kurve I entspricht der Reynold'schen Zahl $R = 10\,000$ ($R = \frac{v d}{\nu}$, v = Windgeschwindig-

keit, d ein lineäres Maß für den betreffenden Körper, $\nu = 0{,}145$ cm²/sec ist die Viscosität), Kurve II entspricht $R = 500\,000$.

Fig. 2: Gesamt-Widerstandszahl c für variierende Werte von R. Der Gesamt-Widerstand P kann dann aus der Formel $P = c \cdot F \cdot nt$ gefunden werden.

Fig. 3: Die Druckverteilung bei einem quadratischen Prisma; in der Tabelle sind für verschiedene Höhen des Prismas mittlerer Druck, Widerstandszahl und innerer Druck (für einen gleichmäßig durchlässigen Körper) angegeben.

Fig. 4: Resultate von Versuchen mit verschiedenen Haustypen; alle Drücke sind als Differenzen des äußeren und inneren Druckes angegeben.

Fig. 5: Druckkurven für verschiedene Dachneigungen einer etwas geänderten Bauform, bei der das Haus durch steife Schirme an den Enden begrenzt war, wodurch die Strömung zweidimensional wurde. Man sieht, wie die Dachneigung von 20° zwischen den flacheren Dächern, die Saugwirkung bekommen, und den schrofferen, welche Druck bekommen, eine Grenzscheide bildet.

Um diese Kurven erklären zu können, hat der Verfasser in Göttingen mit dem in Fig. 4 gezeigten Haustypus, wo die entsprechenden Erscheinungen sich um die Dachneigung von 40° als Grenzscheide gruppieren, Stromlinienversuche gemacht.

Fig. 6 und 7: Entstehung und Entwickelung der Strömung, teils bei 45° Dachneigung und teils bei 30°.

Man sieht, wie beim Dachfirst ein Wirbel entsteht, wie dieser Wirbel abrollt, und daß eine Wirbelfläche vor dem Hause in dem stationären Zustand, an der vordersten Dachtraufe endend, gebildet ist, so wie auch eine Wirbelfläche hinter dem Hause vom Dachfirste ausgehend.

Die vorderste Wirbelfläche gibt die Erklärung der genannten Druckkurven.

Bei 45° Dachneigung ist die Wirbelfläche flacher als die Dachfläche, und man bekommt deshalb Druck am Dache, bei 30° ist sie schroffer (folglich Saugwirkung). Dementsprechend ist in Fig. 5 eine supponierte vorderste Wirbelfläche eingelegt. Man hat sich bis jetzt nur mit der hinteren Wirbelfläche beschäftigt und deswegen geglaubt, daß man Modellversuche auf die Praxis übertragen könne, jetzt aber macht die Feststellung der vorderen Wirbelfläche es wahrscheinlich, daß die Modellgröße die Druckverteilung bei recht flachen Dachneigungen beeinflußt. Diesbezügliche Untersuchungen sind vorgesehen.